PHYSICAL REVIEW E, VOLUME 63, 055202(R)

Spiral waves in a class of optical parametric oscillators

Stefano Longhi
Dipartimento di Fisica, Istituto Nazionale di Fisica per la Materia, Politecnico di Milano, I-20133 Milano, Italy
(Received 27 December 2000; published 16 April 2001)

The formation of three-armed rotating spiral waves is shown to occur in a spatially extended nonlinear optical system with broken phase invariance. These new spatial structures are found in the mean-field model of a class of optical parametric oscillators ($3\omega \rightarrow 2\omega+\omega$) in which the multistep process $2\omega=\omega+\omega$ breaks the phase invariance of the down-conversion process. A parametrically-forced Ginzburg-Landau equation is derived to explain the existence of phase-armed spiral waves.

DOI: 10.1103/PhysRevE.63.055202 PACS number(s): 05.45.Xt, 42.65.Sf

Spiral waves provide a beautiful and generic example of pattern formation in spatially extended systems in diverse fields of nonlinear sciences [1]. In nonlinear optics, since the pioneering work by Coullet and co-workers [2], a large amount of work has been devoted to the study of optical vortices [2–7]. Phase spiral patterns have been shown to be generic to the Maxwell-Bloch laser equations [2–4] and observed in diverse laser systems [5–7]. Optical vortices and spiral waves also arise in optical parametric processes in a nonlinear $\chi^{(2)}$ medium [8–10]. Most of these previous studies were focused on phase invariant systems, where spiral waves manifest usually as phase defects for either scalar or vectorial fields [11]. A different kind of spiral patterns may occur in spatially extended systems with broken phase invariance, where domain walls separating n different phase-locked states may appear and tend to spiral [12]. Armed spiral waves corresponding to $n=2$, 3, and 4 have been shown to be rather generic in periodically forced oscillatory systems and found in the analysis of a forced Ginzburg-Landau equation [12–15]. The simplest and most studied case corresponds to $n=2$, where two kinds of domain walls, Ising and Bloch walls, may separate two equivalent states which differ each other by a π phase shift. In this case stationary Ising walls may lose their stability to a pair of counterpropagating moving fronts (Bloch walls), which may lead to the formation of a two-armed rotating spiral wave [12]. Observation of phase-locked armed spiral waves has been reported in nematic liquid crystals subjected to a rotating magnetic field for $n=2$ [16] and recently in periodically forced reaction-diffusion systems for $n=2$, 3, and 4 [17,18]. In the context of nonlinear optics, Ising-like domain walls connecting two phase states have been found in optical parametric oscillators (OPO) in the degenerate configuration [19], whereas Bloch walls and Ising-Bloch transitions have been recently predicted for a type-II OPO with weak birefringence and dichroism [20]. So far, however, no example of three-armed spiral waves has been reported yet for a nonlinear optical system.

In this Rapid Communication we provide an example of a nonlinear optical system with broken phase invariance which supports three-armed spiral waves. We consider a doubly resonant OPO in a frequency configuration [21] that converts an unresonated plane-wave pump field at frequency 3ω into signal and idler fields at frequencies ω and 2ω, respectively. Owing to the 1:2:3 ratios among the frequencies of interacting fields, two distinct parametric processes may simultaneously occur in the nonlinear $\chi^{(2)}$ crystal: nondegenerate parametric down-conversion of the pump field ($3\omega=\omega+2\omega$) and, as a multistep process, second-harmonic generation ($\omega+\omega=2\omega$) [22]. We assume that the nonlinear crystal is phase-matched for the divide-by-three down-conversion process $3\omega \rightarrow 2\omega+\omega$, i.e., $k(3\omega)=k(2\omega)+k(\omega)$, whereas the multistep parametric interaction, $\omega+\omega=2\omega$, is assumed to be weakly phase-matched with a phase mismatch parameter $\Delta k \equiv k(2\omega)-2k(\omega)$ much larger than π/l, l being the crystal length. The mean-field equations for the normalized amplitudes A_1 and A_2 of intracavity signal and idler fields can be derived starting from the paraxial propagation wave equations for pump, signal and idler fields in presence of the multistep parametric process [22] after the introduction of the single-longitudinal mode approximation and eliminating the pump field from the dynamics as detailed, e.g., in Ref. [23]. This yields:

$$\partial_t A_1 = \gamma_1[-(1+i\Delta_1)A_1 + ia_1\nabla^2 A_1 + \mu A_2^* + \sigma A_1^* A_2 - |A_2|^2 A_1], \tag{1a}$$

$$\partial_t A_2 = \gamma_2\left[-(1+i\Delta_2)A_2 + ia_2\nabla^2 A_2 + \mu A_1^* - \frac{\sigma}{2}A_1^2 - |A_1|^2 A_2\right]. \tag{1b}$$

In Eqs. (1), μ is proportional to the amplitude of the external pump field; (γ_1,γ_2), (a_1,a_2), and (Δ_1,Δ_2) are cavity decay rates, diffraction and cavity detuning coefficients for signal and idler fields, respectively ($\gamma_1 a_1 = 2\gamma_2 a_2$ if signal and idler are resonated in the same cavity); and σ is a dimensionless parameter that measures the strength of the multistep parametric process. Its explicit expression reads $\sigma = (\sigma_2/\sigma_1) f (2\gamma_1 T_R/3)^{-1/2}$, where T_R is the cavity roundtrip time, $f \equiv |\sin(\Delta k l/2)/(\Delta k l/2)|$ is the mismatching parameter for the $2\omega=\omega+\omega$ process, and σ_1,σ_2 are proportional to the elements of the second-order susceptibility tensor for the two parametric processes $3\omega=2\omega+\omega$ and $2\omega=\omega+\omega$, respectively [22]. The order of magnitude of σ largely depends on phase matching conditions; here we consider the case of weak phase matching such that σ is of order ~ 1 or smaller. As compared to the standard mean-field model of a nonde-

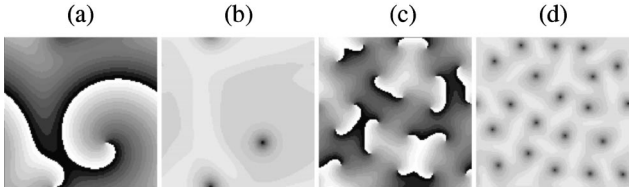

FIG. 1. Spiral waves obtained from numerical simulations of the OPO equations (1) in case of phase invariance ($\sigma=0$). (a),(c) are snapshots of the phase of signal field, and (b),(d) are the corresponding intensity patterns obtained for $\mu=1.3$ at time $t=10\,000$ [(a) and (b)] and for $\mu=2$ at time $t=6000$ [(c) and (d)]. The other parameter values are: $\gamma_1=1$, $\gamma_2=0.5$, $a_1=1$, $a_2=0.3$, $\Delta_1=0.45$, and $\Delta_2=0$ ($\mu_{th}=1.0440$). The equations were integrated using a pseudospectral technique in a square domain of size 50×50 with periodic boundary conditions. A spatial grid of 128×128 points was used; time step $dt=0.02$.

generate OPO (see, e.g., Refs. [9,24]), the multistep parametric process introduces quadratic nonlinear interactions that break the phase invariance of the nondegenerate OPO. The trivial zero solution $A_1=A_2=0$ undergoes an Hopf bifurcation with frequency $\omega_c=\gamma_1\gamma_2(\Delta_2-\Delta_1)/(\gamma_1+\gamma_2)$ to a spatially homogeneous state for signal and idler fields at $\mu=\mu_{th}\equiv(1+\Delta^2)^{1/2}$ when $\Delta>0$, where $\Delta\equiv(\gamma_1\Delta_1+\gamma_2\Delta_2)/(\gamma_1+\gamma_2)$ is the effective detuning parameter. For $\sigma=0$, phase invariance is not broken and defects in the form of optical vortices, corresponding to phase singularities of the fields, can be observed. Frozen states of rotating spiral waves may be found in numerical simulations of Eqs. (1) when $\sigma=0$ and $\Delta>0$ (see Fig. 1). These defect states are analogous to those found in the Maxwell-Bloch laser equations [2] and are consistent with the reduction of the nondegenerate OPO equations to a complex Ginzburg-Landau equation for $\Delta>0$ [25]. For a nonvanishing value of σ, the phase invariance of the OPO equations is broken, the onset of parametric oscillation becomes subcritical, and phase-locked homogeneous states may exist. These states are given by $A_{1,2}=R_{1,2}^{1/2}\exp(i\phi_{1,2})$, where $\phi_1=(\theta_1-\theta_2)/3$, $\phi_2=(2\theta_1+\theta_2)/3$, $\sin\theta_1=(\Delta_1R_1-2\Delta_2R_2)/(\mu^2R_1R_2)^{1/2}$, $\sin\theta_2=2(\Delta_1R_1-2\Delta_2R_2)/(\sigma R_1R_2^{1/2})$, and R_1,R_2 can be found numerically from the solutions of a quartic algebraic equation in $r=R_2/R_1$. The existence of the locked solution requires $\sigma>\sigma_c$, where the critical value σ_c can be found numerically by an analysis of the quartic equation; in particular, it turns out that $\sigma_c=0$ for $\Delta_1=\Delta_2$, i.e., when $\omega_c=0$. For $\sigma<\sigma_c$, the system does not admit of a phase-locked stationary solution, and a limit cycle is found. For $\sigma>\sigma_c$, two possible solutions for (R_1,R_2) can be found from the quartic equation; however, one branch is always unstable to perturbations with zero transverse wave number (see Fig. 2). The stability of the other branch against perturbations with transverse wave number $k\neq0$ can be tested by numerical evaluation of the eigenvalues in the linearized system obtained by linearizing Eqs. (1) around the phase-locked state. In general, we found that the phase-locked homogeneous state is linearly stable and no modulational instabilities could be found for a wide range of parameter values. Notice that, for a given value of (R_1,R_2) in the stable branch, *three* different values

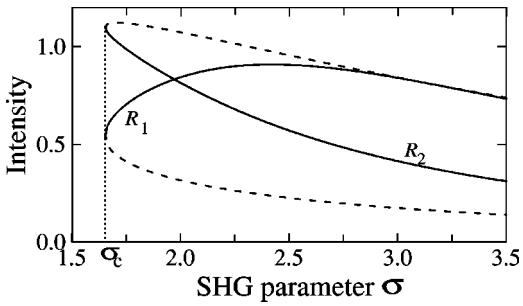

FIG. 2. Behavior of signal (R_1) and idler (R_2) intensities, versus the second-harmonic generation (SHG) parameter σ, corresponding to the homogeneous phase-locked solutions of the OPO equations. Continuous curves denote the stable branch, whereas the dashed ones the unstable branch. Parameter values are: $\gamma_1=\gamma_2=1$, $a_1=1$, $a_2=0.5$, $\Delta_1=1$, $\Delta_2=0.1$, and $\mu=2$. The locked solutions exist for $\sigma>\sigma_c=1.655$, and three phases, which differ by multiples of $\pm2\pi/3$, are possible.

for the phases ϕ_1 and ϕ_2 of A_1 and A_2, which differ from each other by multiples of $\pm2\pi/3$, are possible. This means that the system exhibits three different phase states, and domain walls connecting different phase states are possible. Numerical analysis of Eqs. (1) for $\sigma>\sigma_c$ shows that phase-locked states with different phases may emerge from noise in different spatial regions, which are connected by domain walls that appear as dark lines in the field intensity. Domain walls are generally moving and their dynamics seems to be governed by both curvature effects and by motion of the walls, perhaps due to nonvariational effects. Shrink or expansion of domain walls, leading to a one dominant final phase state, is possible, however, more complex dynamical behaviors can be observed. In particular, stable three-armed rotating spirals can be found in numerical simulations of Eqs. (1) with a flat pump profile starting from a small random noise as an initial condition and assuming periodic boundary conditions (see Fig. 3). Spiral waves are nucleated spontaneously from noise and correspond to three domain walls, that separate three different phase-locked states, coalescing in one point and rotating around this point. Spiral waves with different ordered phase states rotate in opposite directions, and annihilation of counter-rotating spirals may occur. In order to test the robustness of spiral waves under more realistic finite pumping configurations, we considered

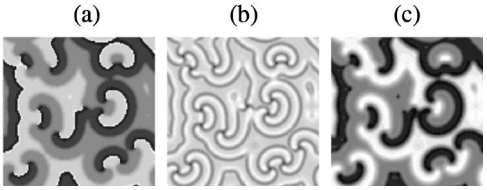

FIG. 3. Rotating three-phase spiral waves of the OPO equations with broken phase invariance (flat pump field, periodic boundary conditions). The figure shows snapshots at time $t=9850$ of the phase [(a)], intensity [(b)], and real-part [(c)] of the signal field $A_1(x,y,t)$. The SHG parameter is $\sigma=2$ ($\sigma_c=1.655$); the other parameter values are the same as in Fig. 2. The computing window is 68×68 on a 128×128 spatial grid; time step: $dt=0.01$.

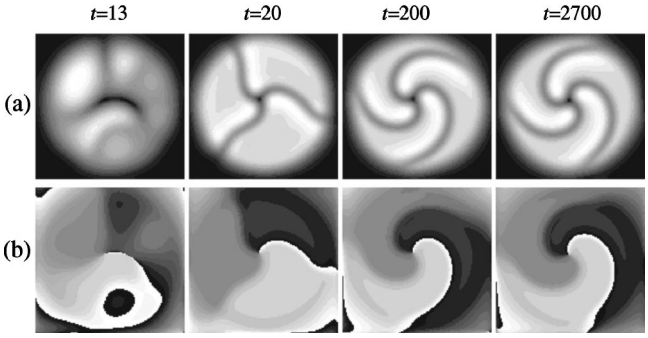

FIG. 4. Snapshots at successive times showing the formation from noise of a rotating three-phase spiral wave for a super-Gaussian pump field ($m=14, r_0=10.45, \mu_0=2$). Parameter values are as in Fig. 3. The box size in 22×22 on a 128×128 spatial grid; time step: $dt=0.01$.

the case of a super-Gaussian pump beam locally flat near the cavity axis with fast decay at the boundary, i.e., we assumed $\mu(x,y)=\mu_0\exp[-(r/r_0)^{2m}]$, where r is the transverse radial coordinate, r_0 the pump beam size, m the order of the super Gaussian, and μ_0 the peak gain. Spontaneous formation of rotating spirals from noise are observed in this case as well (see Fig. 4); remarkably, stable rotating spirals are found even for a simple Gaussian pump (see Fig. 5), which may be of major importance for an experimental observation of spiral waves. Notice also that the circular symmetry of the boundary helps the formation of large spiral structures for large aspect ratios (see Fig. 5); similar boundary-enhanced spiraling was previously reported for both phase and intensity spiral waves in other nonlinear optical systems [10,26]. Well above σ_c, the tendency of spiraling is prevented, and more complex patterns, slowly evolving in time, are observed (Fig. 6). These structures do not arise from a modulational instability, instead they originate from the spontaneous nucleation of bubbles near the domain walls, leading to a characteristic holey tiling in the phase (see Fig. 6). We did not attempt to fully capture the complex dynamical scenario of Eqs. (1) in the whole parameter space; instead, we tried to understand the existence of three-armed rotating spiral waves by the derivation of an order parameter equation close to threshold for $\Delta>0$ and for a small value of the symmetry-

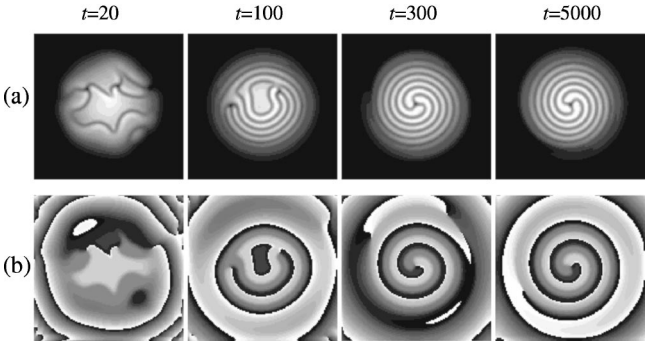

FIG. 5. Same as Fig. 4 but for a Gaussian pump ($m=1, r_0=27$). Parameter values are the same as in Fig. 4 except for $\mu_0=2.3$. The box size in 60×60 on a 128×128 spatial grid; time step: $dt=0.01$.

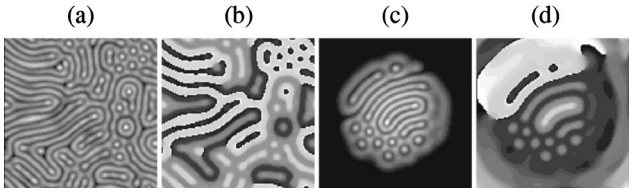

FIG. 6. Snapshots at time $t=6000$ of intensity [(a) and (c)] and phase [(b) and (d)] of holey phase patterns for A_1 in case of a flat [(a) and (b)] and Gaussian [(c) and (d)] pump beam, as obtained for $\sigma=6$. The other parameter values are as in Figs. 3 and 5, except for $r_0=19$. The integration window is 20×20; time step $dt=0.005$.

breaking parameter σ, say $\sigma\sim\epsilon$. Since we are interested in the phase-locked regime, we also assumed a small value for ω_c and of the same order of magnitude as σ, i.e., we assume $\Delta_1\sim\Delta_2$. The amplitude equation for Eqs. (1), close to the bifurcation point $\mu=\mu_{th}$, can be derived as a solvability condition in a multiple-scale asymptotic expansion following the same technique as detailed in Refs. [24,25]. At leading order, one finds that $(A_1,A_2)^T=[1,(1-i\Delta)/\mu_{th}]^T F(x,y,t)+O(\epsilon^2)$, where the amplitude $F\sim\epsilon$ satisfies the following equation:

$$\partial_t F=\alpha F+\beta\nabla^2 F+\rho F^{*2}-\delta|F|^2F, \tag{2}$$

where we have set

$$\alpha=\frac{2\gamma_1\gamma_2\mu_{th}(\mu-\mu_{th})}{\gamma_1+\gamma_2+i(\gamma_1-\gamma_2)\Delta}+i\frac{\gamma_1\gamma_2(\Delta_2-\Delta_1)}{\gamma_1+\gamma_2}, \tag{3a}$$

$$\beta=\frac{i\gamma_1\gamma_2[a_1-a_2-i\Delta(a_1+a_2)]}{\gamma_1+\gamma_2+i(\gamma_1-\gamma_2)\Delta}, \tag{3b}$$

$$\rho=\sigma\frac{\gamma_1\gamma_2(1-3\Delta^2-4i\Delta)}{2\mu_{th}[\gamma_1+\gamma_2+i(\gamma_1-\gamma_2)\Delta]}, \tag{3c}$$

$$\delta=\frac{2\gamma_1\gamma_2}{\gamma_1+\gamma_2+i(\gamma_1-\gamma_2)\Delta}. \tag{3d}$$

After the change of variables $t\to c_1 t$, $\nabla^2\to(1/c_2)\nabla^2$, $F\to c_3F$, with $c_1=1/\mathrm{Re}(\alpha)$, $c_2=\mathrm{Re}(\beta)/\mathrm{Re}(\alpha)$, and $|c_3|^2=\mathrm{Re}(\alpha)/\mathrm{Re}(\delta)$, Eq. (2) reduces to the following parametrically forced complex Ginzburg-Landau equation:

$$\partial_t F=(1+i\nu)F+(1+i\eta)\nabla^2F-(1+i\theta)|F|^2F+pF^{*2}, \tag{4}$$

where $\nu=\mathrm{Im}(\alpha)/\mathrm{Re}(\alpha)$, $\eta=\mathrm{Im}(\beta)/\mathrm{Re}(\beta)$, $\theta=\mathrm{Im}(\delta)/\mathrm{Re}(\delta)$, and $p=|\rho|/[\mathrm{Re}(\alpha)\mathrm{Re}(\delta)]^{1/2}$. In its present form, Eq. (4) describes quite generally the dynamics of an oscillatory system close to an Hopf bifurcation when it is resonantly forced at a frequency 3ω, where ω is its natural frequency [12]. This equation is known to admit of three stable phase states, which differ each other by multiplies of $2\pi/3$, for $p>p_c$, where the critical value for phase locking is given by $p_c=\sqrt{2}[(1+\theta^2)^{1/2}(1+\nu^2)^{1/2}-(1+\nu\theta)]^{1/2}$. Domain walls connecting different phase states are in general moving due to nonvariational effects [15], and three-armed rotating spi-

rals, similar to the ones observed in our numerical simulations, are possible in the phase-locking regime [12,15]. In addition, it is remarkable that these structures are robust against noise and persist for spatially inhomogeneous forcing [14]. Spiral waves observed in our numerical simulations thus bear a close connection with phase-locked armed spiral waves generally observed in resonantly forced oscillatory systems. More complex patterns, such as those observed at large values of the symmetry-breaking parameter σ (see Fig. 6), are not, however, described by the reduced order parameter equation (4), and seem peculiar to the original OPO equations.

In conclusion, three-armed rotating spiral waves have been predicted to exist in a nonlinear optical system with broken phase invariance. We considered an OPO for the frequency down-conversion $3\omega \rightarrow 2\omega + \omega$ in which a weakly phase-matched multistep parametric process allows for multistability of three different phase states. The spiral waves supported by this system are rather distinct from other kinds of phase and intensity spirals previously found in nonlinear optics [2–4,8,10]; instead they bear a close connection with spiral waves found in parametrically forced magnetic and chemical systems [12,17,18].

This work was partially supported by the ''Progetto Giovani Ricercatori'' and by the ESF Network PHASE.

[1] M. C. Cross and P. C. Hohenberg, Rev. Mod. Phys. **65**, 851 (1993).
[2] P. Coullet, L. Gil, and F. Rocca, Opt. Commun. **73**, 403 (1989).
[3] L. Gil, Phys. Rev. Lett. **70**, 162 (1993).
[4] D. Yu, W. Lu, and R. G. Harrison, Phys. Rev. Lett. **77**, 5051 (1996).
[5] F. T. Arecchi, G. Giacomelli, P. L. Ramazza, and S. Residori, Phys. Rev. Lett. **67**, 3749 (1991).
[6] C. O. Weiss, Phys. Rep. **219**, 311 (1992).
[7] K. Staliunas, G. Slekys, and C. O. Weiss, Phys. Rev. Lett. **79**, 2658 (1997).
[8] K. Staliunas, Opt. Commun. **91**, 82 (1992).
[9] V. J. Sanchez-Morcillo, E. Roldan, G. J. de Valcarcel, and K. Staliunas, Phys. Rev. A **56**, 3237 (1997).
[10] P. Lodahl, M. Bache, and M. Saffman, Phys. Rev. Lett. **85**, 4506 (2000).
[11] A notable exception is the analysis of Ref. [10], where intensity spiral waves are observed in an internally pumped optical parametric oscillator as a result of a secondary instability.
[12] P. Coullet and K. Emilsson, Physica D **61**, 119 (1992).
[13] C. Elphick, A. Hagberg, and E. Meron, Phys. Rev. Lett. **80**, 5007 (1998).
[14] C. J. Hemming and R. Kapral, Chaos **10**, 720 (2000).
[15] R. Gallego, D. Walgraef, M. San Miguel, and R. Toral (unpublished).
[16] T. Frisch, S. Rica, P. Coullet, and J. M. Gilli, Phys. Rev. Lett. **72**, 1471 (1994).
[17] A. L. Lin, M. Bertram, K. Martinez, H. L. Swinney, A. Ardelea, and G. F. Carey, Phys. Rev. Lett. **84**, 4240 (2000).
[18] A. L. Lin, A. Hagberg, A. Ardelea, M. Bertram, H. L. Swinney, and E. Meron, Phys. Rev. E **62**, 3790 (2000).
[19] S. Trillo, M. Haelterman, and A. Sheppard, Opt. Lett. **22**, 970 (1997).
[20] G. Izus, M. San Miguel, and M. Santagiustina, Opt. Lett. **25**, 1454 (2000).
[21] See, for instance, A. Douillet and J.-J. Zondy, Opt. Lett. **23**, 1259 (1998).
[22] K. Koynov and S. Saltiel, Opt. Commun. **152**, 96 (1998); Y. S. Kivshar, T. J. Alexander, and S. Saltiel, Opt. Lett. **24**, 759 (1999).
[23] S. Longhi, J. Mod. Opt. **43**, 1089 (1996); P. Lodahl and M. Saffman, Phys. Rev. A **60**, 3251 (1999).
[24] S. Longhi, Phys. Rev. A **53**, 4488 (1996).
[25] Z. H. Musslimani, Physica A **249**, 141 (1998).
[26] I. Aranson, D. Hockheiser, and J. V. Moloney, Phys. Rev. A **55**, 3173 (1997).